ELSEVIER

Thermochimica Acta 319 (1998) 151–162

thermochimica acta

Design improvements in adiabatic calorimetry The heat capacity of cholesterol between 10 and 425 K

J.C.van Miltenburg*, A.C.G.van Genderen, G.J.K.van den Berg

Department of Interfaces and Thermodynamics, Utrecht University, Padualaan 8, 3584 CH Utrecht, The Netherlands

Received 6 September 1997; accepted 1 June 1998

Abstract

Design improvements in an adiabatic calorimeter are described. The changes make it possible to load or unload the calorimeter in half an hour. A new regulation system is discussed and changes in the data collection and the data calculation programs are given. The molar heat capacity of cholesterol has been measured between 5 and 425 K. The derived thermodynamic properties are calculated. The solid–solid transition was found at 306.7 K, with an enthalpy of transition of 3886 J mol^{-1}. The melting temperature was found to be 422.3 K, the enthalpy of fusion being 28.4 kJ mol^{-1}. © 1998 Elsevier Science B.V.

Keywords: Adiabatic calorimetry; Cholesterol; Thermodynamic properties

1. Introduction

In 1987, we published the design and construction of an adiabatic calorimeter [1]. Special attention was paid to economical use of liquid helium and to easy mounting and dismounting of the sample container. This calorimeter, with some adaptations, has been in use till today. The major adaptation in the original design was the removal of the conical heat contacts between the vessel and the shields. The vessel could be lifted from the outside by a windlass, resulting in a direct metallic contact with the liquid helium container. A second possibility for quick cooling, which was also contained in the first version, was the separate vacuum space surrounding the vessel and the adiabatic shields. By breaking this vacuum with helium gas quick cooling was possible without excessive losses of the coolant liquid. This second method proved to be mostly used in practice, and the more accident-prone metallic heat contacts, which also contributed unfavorably to the heat capacity of the shields and the vessel, were removed.

More recently (1994) a new measuring program was written and the whole system was reconsidered. A second adiabatic calorimeter was taken into use. In this article, we want to discuss the changes in hardware and software and present the results of the heat-capacity measurements of cholesterol from 10 to 425 K. We have chosen cholesterol, as it is an important biological compound of which no thermal data in this range are available.

*Corresponding author. Tel.: 0031-30-2532386; fax: 0031-30-2533946; e-mail: mitenb@chem.uu.nl

PII S0040-6031(98)00402-X

2. Experimental

2.1. Hardware improvements

The adiabatic calorimeter consists of a sample container, equipped with a thermometer and a heater, surrounded by shields of which the temperature is precisely controlled with respect to the temperature of the sample container. The use of high vacuum (in the order of 5×10^{-5} Pa) and gold plating reduces the heat exchange by conduction and radiation between the adiabatic shields and the sample container. The heat conduction along the wires needed for temperature measurement and electrical heating is kept small by using thin wires and is controlled by a separate heating system which brings the wires to the temperature of the sample container. The calorimeter is mounted under the liquid helium tank of the cryostat. A schematic drawing of the apparatus is given in Fig. 1. As very thin wires are used (Litze wire 7×0.01 mm), the system is easily damaged by a wire rupture. Repairs in situ are not easy and we decided to use mini connectors, soldered to the heat-conduction pins at the bottom of the liquid helium tank. In case of damage, the whole calorimeter part can be separated from the cryostat and repaired on the work-bench. We have not found any influence of the added connections on the quality of the data.

The radiation shields were made of copper and over the years they lost their original shine. Gold plating of these shields and soldering the double radiation shield to the bottom of the liquid nitrogen tank (see insert in Fig. 1) greatly reduced the use of liquid nitrogen. The soldering of both shields to the liquid nitrogen tank directs all incoming radiation heat to the nitrogen tank and ensures that the liquid helium tank is surrounded by a shield at liquid nitrogen temperature. Complete filling of both the tanks with liquid nitrogen allows for a 7 days working period between 80 and 300 K without refilling. When liquid helium is used in the lower tank, ca. 5 l are used to cool down the system from 80 to 5 K and two working days are available without refilling.

The separate vacuum space surrounding the calorimeter compartment was closed in the original design by soft soldering (woods metal) of the shield (number 10 Fig. 1) to the copper ring at the bottom of the helium tank. This ring also contains the heat-contact pins for the wires (see insert). The soldering process raised the temperature of the sample to ca. 325 K. This could give unwanted melting of the compound and the soldering process took ca. 1 h. Another drawback was the manipulating of the heating elements needed, the fragile wires of the calorimeter could easily be broken. We replaced this system by a vacuum closure which is obtained by compressing a large Teflon ring. (ca. 12 cm diameter, with an oval cross section) This is comparable to an O-ring closure, but the low temperatures complied us to use Teflon. This closure proved to be sufficiently vacuum tight. After admitting helium gas in the separate vacuum space, some leakage could sometimes be observed, but cooling to the intended temperature was always possible. The splitting of the radiation shield coming from the liquid nitrogen tank (number 14 Fig. 1) is now done with a bayonet-catch instead of flanges. This also facilitates the mounting and demounting of the vessel. With these changes it takes about half an hour to mount the calorimeter vessel.

2.2. The calorimeter vessel

The calorimeter vessel should be chemical resistant, has a good heat conductivity, must be easy to clean, has a relatively small mass and must be durable. In the design given in Fig. 2, these objects were realized. It is made of copper, electrically gold-plated on the outside and gold-plated on the inside by a chemical method. The top part of the vessel is flanged, thus omitting a soldering connection and improving the smoothness of the inside of the vessel. The soldering connections were made with Ag(65)-Pd(15)-Cu(20) solder, melting range 850–900°C in a hydrogen oven. The mass of the total vessel, including the gold plate and the screw cap is ca. 20 g. The volume is 11 ml. When measuring the heat capacity of this vessel, the transient time after an input period, needed for the redistribution of the supplied heat, is in the order of 60 s.

2.3. The wire heater

The wire heater is situated between the first and the second adiabatic shield. The temperature is regulated with respect to the temperature of the vessel, using a copper–constantan thermocouple.

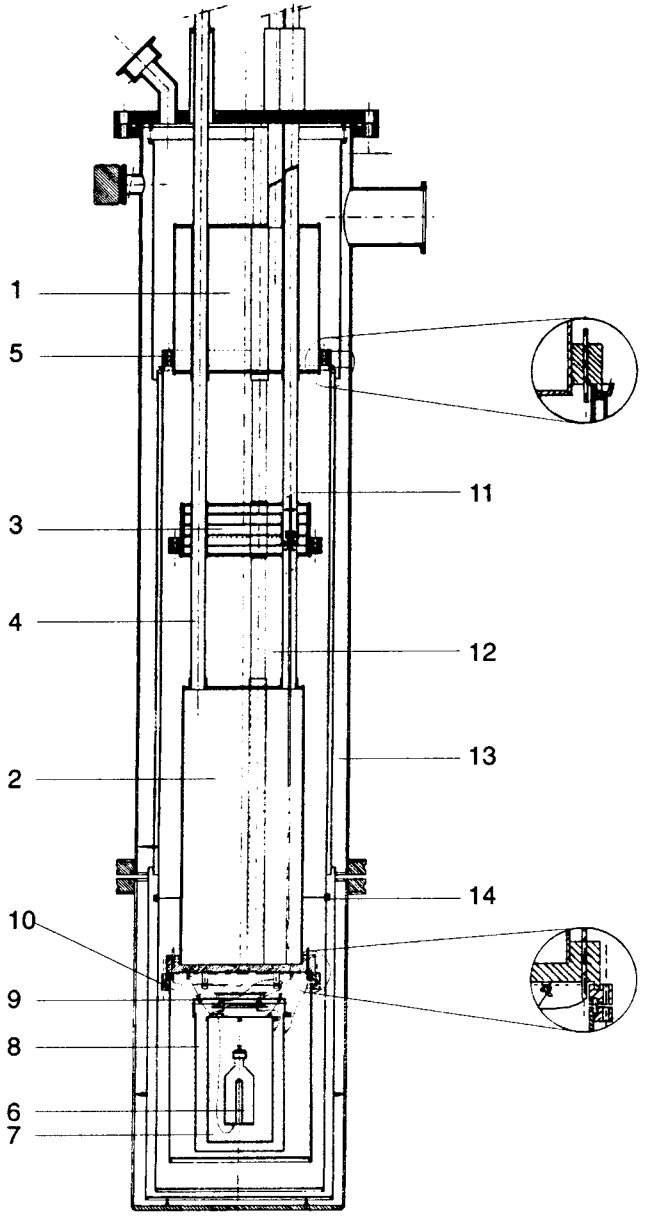

Fig. 1. The adiabatic calorimeter. Legend: 1, liquid nitrogen tank; 2, liquid helium tank; 3, economizer, after lowering the plunger (11) the gas is forced to circulate between the plates; 4, filling tubing liquid helium; 5, ring with heat-contact pins for soldering the incoming wires (see also the enlargement); 6, vessel with insert; 7, first adiabatic shield; 8 s adiabatic shield; 9, wire heater; 10, vacuum closure of the calorimeter compartment (see also enlargement); 11, plunger for closing the direct escape route of the helium gas; 12, tube for evacuating the calorimeter compartment; 13, double radiation shield, gold plated and connected to the liquid nitrogen tank.; 14, bayonet-catch for separating radiation shield.

We use two designs for the wire heater, the first was already described in 1987 [1], it consists of a copper disk, equipped with a heating wire and heat-contact pins of lacquered copper wires. The new design in the second adiabatic calorimeter is simpler. The thermocouple is lacquered in the center of the wire bundle, a

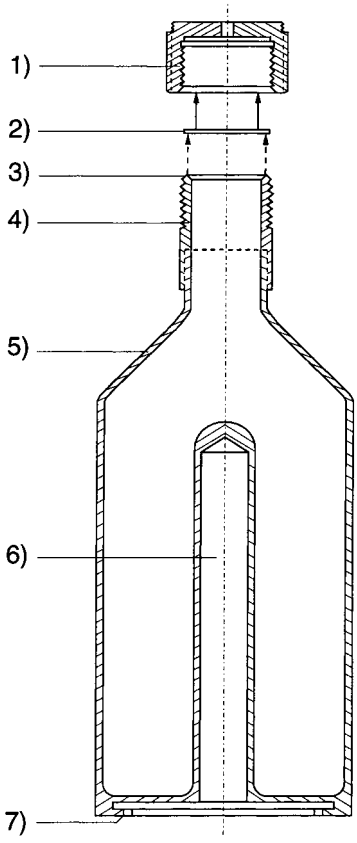

Fig. 2. The vessel. Legend: 1, screw cap; 2, gold plate, 0.4 mm thick; 3, sharp edge, 45°; 4, sparkal neck (70% Cu-30% W); 5, flanged side (by cold rolling); 6, re-entrant well for thermometer and heater assembly; 7, bayonet-catch for forcing the insert against the flat bottom.

heating wire is turned around the bundle (ca. 100 Ω) over a distance of 5 cm and also lacquered. The time constant of this system is very small, as is its heat capacity. This results in a fast response to the regulation. Both systems work adequately.

2.4. The temperature regulation system

The analogue amplifiers of the original system were replaced by a digital multimeter equipped with a channel selector. (Keithley 2010) The voltage of the thermocouples between the vessel and the inner shield, between the inner and outer shield and between the vessel and the wire heater are measured to within 0.1 μV. The channels are read every 2 s, the data are collected by a computer dedicated to the regulation system and used to calculate the signals for the Digital/Analoque converter (an 8 channel, 12 bits card). The difference ΔV between the actual measured voltage and the set-point of the control is used to calculate $D/A = \sqrt{\Delta VP + I \sum \Delta V}$ in which P is a proportional factor and I the integral factor. The *D/A* signal is used in a 8-channel home-built current amplifier fed by a 50 V DC source.

Each channel can be followed graphically. Settings for separate temperature regions and for the two calorimeters are stored and retrieved when needed. This leads to a higher reproducibility of the measurements. The regulation patterns are symmetrical. The maximum deviations are in the order of 0.2 μV during switching on or off of the sample heater. One channel of the channel selector is short-circuited and is used as 'zero' for all channels. The program is written in Pascal and is available on request.

2.5. Software

The measuring procedure consists of repeating stabilization and input periods. During the stabilization period the temperature is measured as a function of time, during the input period the energy dissipated in the vessel is registered.

A new measuring program written in Pascal gives us more flexibility in how to perform a measurement. The main advantages are:

– A pick file is re-written each time a new series of measurements is started. Starting the next run this file is read and only small changes are needed.
– The operator may choose to store the time–temperature data from each equilibration period. This is especially useful for relaxation processes.
– Two AC-bridges for temperature measurements are used (the ASL A17 and the Tinsley Senator bridge) and can be chosen from the program itself.
– The larger storage capacity of the modern computer allows us to collect more data, roughly every second a temperature measurement is made. This results in a reduced standard deviation of the time–temperature relation in the stabilization periods. We use the second half of the stabilization period to calculate the temperature drift, by fitting the data to a straight line. The standard deviations

range from 10–20 μK between 30 and 100 K to ca. 25–50 μK between 100 and 420 K. Generally the Senator bridge, which is used with a Iron–Rhodium thermometer (Oxford Instruments) gives a slightly lower standard deviation.

– The home-built current source was replaced by a commercial one (Keithley 220). The heat input period can be programmed to follow a stepwise increment and at the end of the period a decrement of the power dissipated. The total period is divided in a main period (mostly 400 to 600 s) and two for and after periods, during which for instance 60 and 30% of the power of the main period is dissipated during 100 and 50 s. The length of these periods can be chosen freely. This symmetrical stepwise delivery of energy has the advantage that the shields can follow the temperature of the vessel closer and, especially, that the temperature overshoot at the end of a heating period becomes much smaller. This overshoot is largely due to the redistribution of the heat delivered in the heating period. The thermocouples are attached to the insert which is equipped with the heater and the thermometer. After a heating period, the temperature of this insert decreases by ca. 0.1 K. As the shields are highly insulated they cannot follow this decrease in temperature in a short time period. The stepwise delivery of the energy reduces the temperature decrease and the shields are normally back in regulation within 50 to 100 s. The program adepts the current needed for the intended temperature increment. This current can be clipped by a maximum and a minimum value. When these values are chosen equal the same amount of energy is dissipated in each input period.

– A separate program '*t*-follow' is used to measure and collect time–temperature data in long stabilization periods. The operator can choose the time between storing the points on the hard disk.

2.6. The calculation programs

Two calculation programs are in use, the first uses the collected data consisting of the temperature at the mid-point of the stabilization period, the slope of the temperature time curve in the second half of the stabilization period dT/dt, the energy supplied and the times t_1 and t_2, being the start and end time of the input period. From these data, the heat capacity of the vessel and its contents are calculated.

When no enthalpy relaxation or other processes, such as melting or crystallization, take place during the measurement, the temperature increase of the vessel is calculated by extrapolating the temperature drifts of the for and after period till the mid-point of the heating period. The heat capacity is then calculated by dividing the supplied energy through this temperature increase. The heat capacity of the empty sample container is measured and calculated in the same way. These data are used to subtract the value of the empty container and the molar heat capacities are calculated. In principle, the same method can be used when enthalpy relaxation in the sample takes place. However, if one wants to calculate the actual enthalpy increment, one has to extend the stabilization periods to very long times. In a melting process, it may take up to 4 h or more before equilibrium is reached. In these cases, we use the heat exchange with the surroundings. This heat exchange is calculated by multiplying the temperature drift by the mean heat capacity of the vessel and its contents before and after the stabilization period. These heat-exchange values are quite reproducible, normally to within 10 μW. In the part of the measurement, where the temperature drift in the stabilization periods are influenced by the process in the vessel, we can use the heat exchange as measured with the empty vessel. These values are first fitted in a simple polynomial function. This option is called 'forced leak'. An alternative method is using the heat-exchange values before and after the process and interpolates them linearly. This method is called 'support points'. Integration of the heat-capacity data calculated by the 'forced leak' method gives the actual enthalpy path followed by the sample container and its contents under the experimental conditions. All energy supplied either by electrical means or heat exchange with the surroundings is accounted for. Calculation of the same data set, for instance in a glass-transition region, by using the extrapolation of for and after periods, gives the temperature increments due to the heat-capacity part of the enthalpy change alone. In oscillating DSC this is generally called the reversible part of the heat capacity. The effect of the enthalpy relaxation or enthalpy recovery is eliminated by the extrapolation. An example is given in Fig. 3. Here, the glass transition in triphenylphosphite [2] is

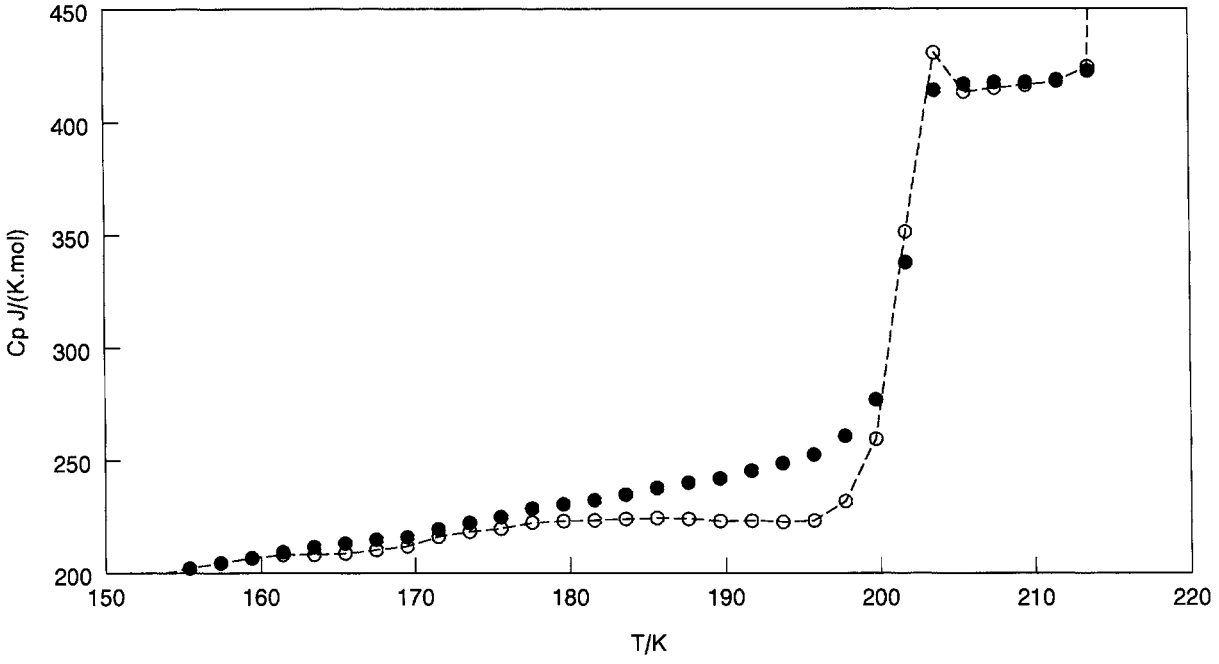

Fig. 3. The glass-transition region of triphenylphosphite. Closed circles, heat capacity calculated by extrapolation of the stabilization periods; open circles, heat capacity calculated by using the known heat exchange with the surroundings.

calculated by the two methods. The open circles show the heat capacity as calculated by using the 'forced leak'. The enthalpy relaxation diminishes the heat capacity just before the glass transition, the enthalpy recovery at the end of the transition increases the heat capacity. These values are dependent on the heating rate. The calculation method with the extrapolation of for and after periods (closed circles) does not take into account the enthalpy relaxation or recovery and gives the 'pure' heat capacity, independent of the heating rate. Calculating the heat-capacity data, in this way, is also useful when a melting process is partially obscured by a slow recrystallisation to a more stable crystal. In this case, the temperature drift due to the recrystallisation can be excluded by extrapolating the observed time–temperature relations.

The second program is used to connect series of measurements, interpolate data at every degree and calculate the derived thermodynamic properties: $H^0(T)-H^0(0)$ and $S^0(T)-S^0(0)$. Furthermore, the program contains an integration routine which calculates a base line using the relative contributions of the heat capacities of the for and after period by an iterative way. Calculation of the purity from melting processes, assuming eutectic behavior of the impurity is possible.

2.7. Performance

The reproducibility of the heat-capacity data is good. Fitting the data of the empty vessel with a polynomial function results in maximum standard deviations of 1% between 5 and 30 K, 0.05–0.1% between 30 and 100 K and 0.03% above 100 K.

The calorimeter was checked using synthetic sapphire between 80 and 400 K [3,4]. No deviations from the recommended values >0.2% were found.

2.8. Chlolesterol

Anhydrous cholesterol was bought from Sigma. The product was used as received. Measurements were made with 3.9427 g (0.0102 mol). The experimental data series are given in Table 1. Series 1 to 9 were all made on the powdery substance as received, in series 9 the product was melted, which had a large influence on the solid-state phase transition. The heat-capacity data

Table 1
Experimental molar heat capacities of cholesterol in chronological order

T/K	C_p/(J K^{-1} mol^{-1})	T/K	C_p/(J K^{-1} mol^{-1})	T/K	C_p/(J K^{-1} mol^{-1})	T/K	C_p/(J K^{-1} mol^{-1})
Series 1							
82.03	168.74	92.71	189.46	103.89	210.46	115.24	231.61
85.34	175.24	96.41	196.53	107.65	217.42		
89.02	182.37	100.14	203.64	111.44	224.61		
Series 2							
301.12	591.36	310.33	711.94	319.56	768.25	329.25	668.12
301.66	593.13	311.28	767.55	320.51	750.32	330.24	660.57
302.43	596.27	312.20	833.08	321.47	736.49	331.23	654.34
303.43	601.63	313.10	880.83	322.43	724.85	332.23	647.82
304.42	607.39	314.00	897.85	323.39	714.57	333.23	642.69
305.42	613.46	314.90	888.24	324.36	706.62	334.23	640.99
306.41	622.31	315.81	867.30	325.33	698.13	335.24	641.82
307.40	633.20	316.74	840.93	326.30	691.103		
308.39	647.50	317.67	813.09	327.28	683.87		
309.37	672.57	318.61	788.44	328.26	675.95		
Series 3							
6.11	3.49	11.18	11.99	17.11	25.14	24.16	41.42
7.72	5.48	13.12	16.05	19.33	29.27	26.50	48.53
9.55	7.78	15.08	21.25	21.71	35.65	28.50	54.41
Series 4							
6.56	3.21	11.34	12.01	17.41	25.67	24.54	42.51
7.98	5.96	13.41	16.15	19.67	30.14	26.85	49.90
9.59	9.11	15.38	22.07	22.07	36.86	28.80	55.28
Series 5							
32.48	65.02	45.16	93.07	61.23	126.14	75.20	154.66
33.85	67.78	48.27	99.67	64.34	132.50	77.64	161.38
36.11	73.34	51.44	106.22	67.26	138.51	80.00	164.23
39.20	80.20	54.68	112.66	70.02	144.30	82.28	168.75
42.16	86.79	57.97	119.42	72.66	150.41	84.49	173.36
Series 6							
93.27	190.93	101.87	208.13	112.47	228.60	122.38	247.02
95.27	194.99	105.50	214.89	115.83	234.99		
98.14	200.59	109.02	221.90	119.14	241.13		
Series 7							
132.59	264.86	178.21	345.68	220.48	423.55	259.31	500.03
134.14	267.53	180.82	350.47	222.85	428.18	261.50	504.94
136.40	272.09	183.41	354.39	225.21	432.69	263.69	509.48
139.39	277.58	185.98	359.66	227.56	437.16	265.87	514.01
142.34	282.69	188.54	364.33	229.89	441.75	268.04	518.54
145.26	287.67	191.08	368.62	232.22	446.20	270.21	523.37
148.14	292.62	193.60	373.57	234.53	450.70	272.37	527.93
151.00	297.28	196.11	378.41	236.83	455.20	274.52	532.90
153.83	302.20	198.61	382.65	239.12	459.78	276.66	537.94
156.63	307.49	201.09	387.34	241.41	464.28	278.79	543.20
159.40	311.88	203.56	391.75	243.68	468.89	280.92	548.74
162.16	315.93	206.01	396.21	245.94	473.24	283.03	554.53
164.88	320.73	208.45	401.13	248.19	477.86	285.14	561.15

Table 1 (*Continued*)

T/K	C_p/(J K^{-1} mol^{-1})	T/K	C_p/(J K^{-1} mol^{-1})	T/K	C_p/(J K^{-1} mol^{-1})	T/K	C_p/(J K^{-1} mol^{-1})
167.59	325.47	210.88	405.69	250.43	482.45	287.22	568.53
170.28	330.22	213.30	410.49	252.66	486.70	289.30	574.05
172.94	334.80	215.70	414.55	254.89	491.19	291.37	578.56
175.58	340.51	218.10	418.80	257.10	495.56		
Series 8							
297.01	584.24	312.04	828.69	328.02	634.87	343.88	653.75
298.95	600.09	314.03	727.87	330.00	635.58	345.86	657.48
300.88	613.91	316.09	677.94	331.98	636.96	347.85	661.09
302.83	631.91	318.11	655.08	333.96	638.12	349.84	664.57
304.77	663.86	320.10	644.72	335.94	640.66	351.82	668.41
306.66	734.92	322.08	639.40	337.93	643.80	353.81	672.44
308.46	882.82	324.06	636.81	339.91	647.05	355.80	675.85
310.20	934.37	326.04	635.01	341.89	650.31		
Series 9							
356.92	679.47	373.25	707.52	391.11	737.96	408.98	767.73
357.89	680.84	375.24	711.42	393.09	741.28	410.97	771.45
359.37	683.41	377.22	714.19	395.08	744.70	412.96	775.06
361.36	687.34	379.20	718.03	397.06	748.45	414.95	778.78
363.34	691.59	381.19	720.72	399.05	751.49	416.94	783.69
365.32	694.24	383.17	723.95	401.03	754.59	418.92	795.19
367.30	698.35	385.15	727.81	403.02	758.14	420.74	1173.05
369.28	701.90	387.14	731.21	405.00	761.58	424.44	936.75
371.27	704.32	389.12	734.63	406.99	764.87		
Series 10							
300.89	535.71	313.70	594.97	326.66	617.12	339.57	641.70
301.80	561.94	314.70	596.79	327.65	618.86	340.56	639.78
302.75	570.03	315.70	599.90	328.64	620.34	341.55	645.38
303.74	574.19	316.69	601.14	329.64	622.99	342.54	647.66
304.74	576.87	317.69	602.60	330.63	624.97	343.53	649.37
305.73	578.72	318.69	604.08	331.63	627.35	344.52	650.92
306.73	581.42	319.69	606.19	332.62	629.50	345.51	653.31
307.73	584.27	320.68	608.08	333.61	630.63	346.51	654.17
308.72	585.82	321.68	609.22	334.61	633.02	347.50	654.96
309.72	587.12	322.68	611.00	335.60	634.25	348.49	658.41
310.72	589.48	323.67	613.25	336.59	635.29	349.48	660.48
311.71	592.39	324.67	614.76	337.59	637.70	350.47	661.78
312.71	593.86	325.66	615.88	338.58	639.97		
Series 11							
122.43	239.60	163.52	314.96	204.89	391.95	246.36	473.99
125.35	245.22	166.47	320.22	207.85	397.82	249.32	479.89
128.28	250.76	169.42	325.56	210.81	403.78	252.28	485.60
131.21	256.22	172.37	330.63	213.77	409.29	255.25	491.40
134.13	261.58	175.33	336.71	216.73	414.37	258.22	497.27
137.06	267.02	178.28	342.44	219.69	420.39	261.18	503.15
139.99	272.45	181.24	347.75	222.65	426.51	264.14	509.21
142.92	277.70	184.19	352.37	225.62	432.46	267.11	515.03
145.86	282.99	187.15	358.53	228.58	438.49	270.07	521.06
148.80	288.31	190.10	363.76	231.54	444.39	273.04	527.44
151.74	293.65	193.06	369.40	234.50	450.39	276.01	533.55
154.68	299.19	196.02	375.35	237.46	456.12	278.98	539.94

Table 1 (*Continued*)

T/K	C_p/(J K^{-1} mol^{-1})	T/K	C_p/(J K^{-1} mol^{-1})	T/K	C_p/(J K^{-1} mol^{-1})	T/K	C_p/(J K^{-1} mol^{-1})
157.63	305.10	198.98	381.04	240.42	462.12		
160.57	309.75	201.93	386.16	243.39	468.03		
Series 12							
281.04	542.03	301.23	606.57	322.00	615.68	343.99	655.26
281.91	545.33	303.19	627.10	324.00	618.69	345.99	658.86
283.34	549.28	305.13	683.82	326.00	621.59	347.99	662.51
285.34	553.24	306.68	1792.16	328.00	625.49	349.99	666.05
287.33	558.00	307.88	1763.03	330.00	628.92	351.99	670.13
289.32	563.34	309.57	745.57	332.00	632.63	353.99	674.19
291.31	568.54	311.79	652.48	334.00	636.35	355.99	677.74
293.29	574.03	313.95	628.31	336.00	639.98	357.99	681.90
295.28	579.93	315.99	618.98	338.00	643.44	359.99	685.95
297.26	586.49	318.00	615.53	340.00	647.41		
299.25	595.02	320.00	615.15	342.00	651.25		

collected in the neighborhood of the phase transition are given in Fig. 4. The phase transition is easily supercooled as can be seen in series 10 (Fig. 4 closed dots). The heat-capacity data, in this series, correspond to the high-temperature phase. It was necessary to cool the solid to 270 K to obtain the low-temperature phase within the time span of these measurements. After cooling again till 80 K, series 11 and 12 were made. The phase transition had sharpened and was shifted to a lower temperature. The enthalpy of transition and the temperature of the maximum in the heat-capacity curves are given in Table 2.

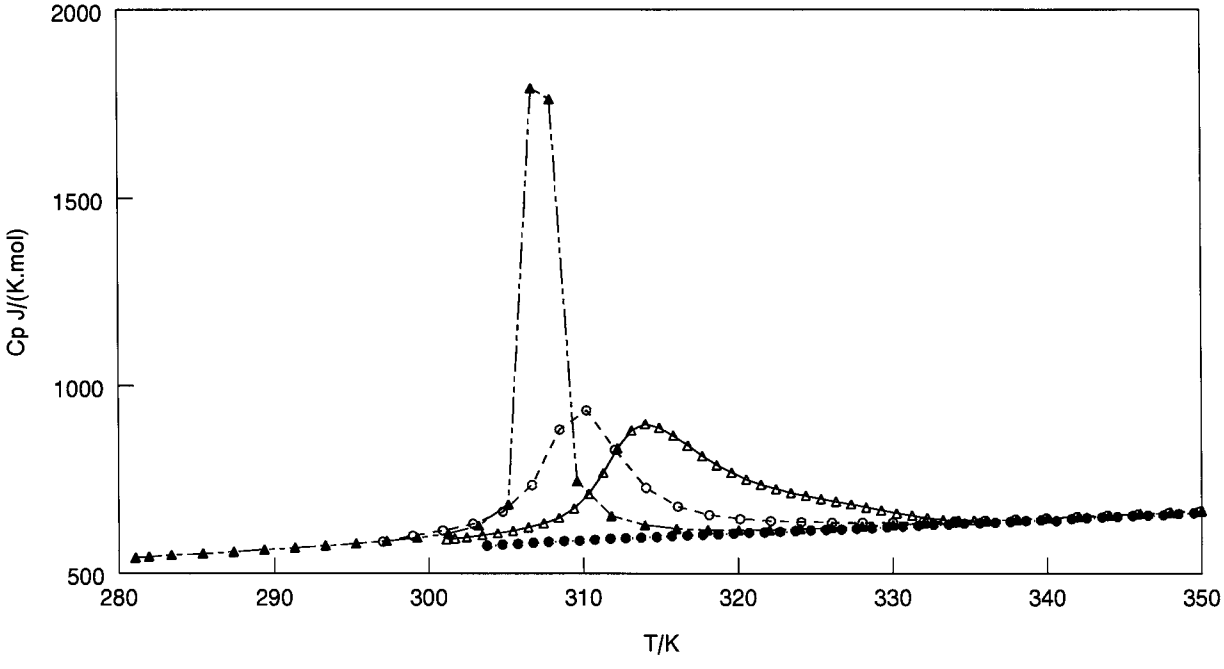

Fig. 4. The transition region of cholesterol. Open triangles, first run, open circles, after cooling till 4 K, but not melted, closed circles, undercooled high-temperature phase, closed triangles, after melting and cooling till 80 K.

Table 2
The enthalpy of transition and the transition temperature

Series	Used calculation range/K	Temperature of the maximum/K	Enthalpy of transition/(J mol^{-1})	Remarks
2	301–335	314	3550	powder as received
8	297–339	310.2	3004	not completely recrystallized
12	281–339	306.7	3886	after melting

From the fractional melting experiment, we calculated an enthalpy of melting of 28430 J mol^{-1} and a purity of 98.8%. The melting temperature, 422.3 K, is very close to the maximum working temperature of the calorimeter, so the melting process was performed only once and we have only one reliable heat-capacity point in the liquid phase.

In Table 3, the derived thermodynamic properties are given. The calculation was started at 10 K, below 10 K a Debye like behavior was assumed, with $Cp = 0.0103T^3$.

The total heat-capacity curve of the solid phase is given in Fig. 5. Except for the transition region, the data between 20 and 420 K are very close to a straight line and can be represented to within a few percent by the following equation:

$$Cp(20\text{–}400\,\mathrm{K}) = 4.8 + 1.897T.$$

Comparing the results with literature data is limited to the solid-state phase transition, which was measured by Petropavlov et al. [5]. They published a value of 2500 J mol^{-1} for the enthalpy of transition, which is low compared to the values we found (see Table 2). There is also a discrepancy in the temperature of transition, they found 304.8 K, our values are between 306 and 314 K. The Nist-databank [6] does contain information about the enthalpy of formation and sublimation, but, except for the enthalpy of transition, no further thermal quantities are mentioned.

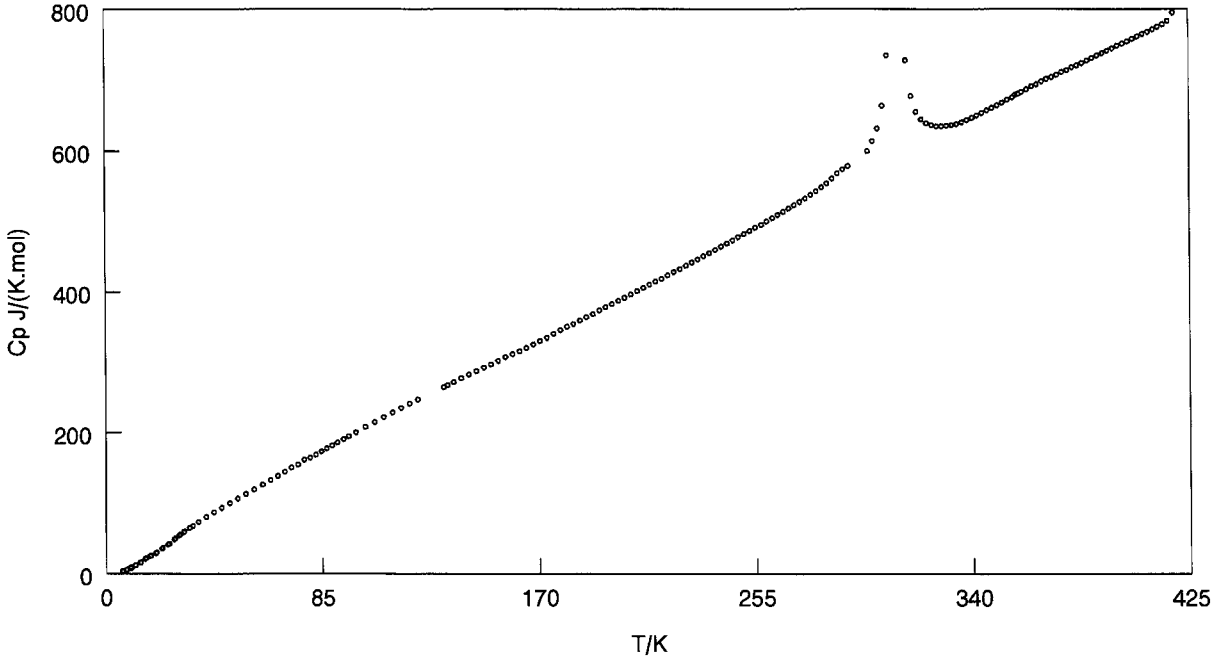

Fig. 5. The molar heat capacity of cholesterol between 10 and 420 K.

Table 3
Thermodynamic properties at selected temperatures for cholesterol (M =386.6616 g mol^{-1} $\Phi_m^0 \stackrel{def}{=} \Delta_T^0 S_m^0 - \Delta_0^T H_m^0/T$)

T/K	C_{pm}^0 /(J K^{-1} mol^{-1})	ΔS_m^0 /(J K^{-1} m ol^{-1})	ΔH_m^0/(J mol^{-1})	Φ_m^0/(J K^{-1} mol^{-1})
10	10.32	3.71	27	0.97
20	31.01	17.01	232	5.45
30	58.42	34.68	677	12.14
40	81.97	54.83	1383	20.26
50	103.28	75.44	2310	29.23
60	123.62	96.05	3444	38.67
70	144.26	116.66	4783	48.33
80	164.25	137.30	6334	58.15
90	184.36	157.80	8073	68.09
100	204.35	178.29	10018	78.11
110	223.80	198.67	12161	88.12
120	242.71	218.97	14492	98.17
130	260.34	239.07	17009	108.27
140	278.63	259.02	19704	118.32
150	295.64	278.86	22573	128.37
160	312.73	298.50	25620	138.39
170	329.75	317.95	28829	148.36
180	349.00	337.32	32221	158.34
190	366.75	356.66	35797	168.24
200	385.31	375.95	39559	178.17
210	404.06	395.17	43503	188.03
220	422.62	414.50	47637	197.89
230	441.95	433.45	51960	207.71
240	461.67	452.78	56476	217.54
250	481.39	472.11	61193	227.32
260	501.50	491.45	66108	237.10
270	522.77	510.78	71227	246.88
280	546.35	530.11	76571	256.67
290	575.74	549.83	82181	266.41
298.15	597.01	566.07	86952	274.41
300	606.67	569.94	88066	276.19
310	941.13	593.14	95254	286.01
320	644.95	616.73	102620	296.03
330	635.67	636.44	108992	306.04
340	647.27	655.39	115395	316.02
350	665.06	674.34	121953	325.99
360	684.78	693.28	128704	335.93
370	702.95	712.62	135645	345.87
380	719.19	731.56	142752	355.77
390	736.20	750.12	150025	365.63
400	752.83	769.07	157472	375.49
410	770.02	787.87	165087	385.22
420	786.99	806.63	172872	395.03
422.33	790.94	811.00	174711	397.31
422.33	936.49	878.27	203122	397.31
425	936.88	884.17	205623	400.35

3. Discussion

The changes in hardware and software have lead to a reliable and easy to use calorimeter, which produces very accurate results. The adiabatic method is still more time consuming than differential scanning techniques, but the results are often more precise and additional information about the thermal behavior in the stabilization periods is important in relaxation processes.

Acknowledgements

The authors wish to express their thanks to Dr. P.R. van der Linde for writing the data collection program.

References

[1] J.C. van Miltenburg, G.J.K. den Berg, M.J. van Bommel, J. Chem. Thermodynamics 19 (1987) 1129.
[2] K. van Miltenburg, K. Blok, J. Phys. Chem. 100 (1996) 16457.
[3] National Bureau of Standards Certificate, Standard Reference Material 720. U.S. Department of Commerce, 1982.
[4] D.G. Archer, J. Phys. Chem. Ref. Data 22 (1993) 1441.
[5] N.N. Petropavlov, I.G. Tsygankova, A.L. Teslenko, Sov. Phys. Crystallogr. 33(6) (1988) 853.
[6] NIST Chemistry WebBook, http://webbook.nist.gov.